Organic & Biomolecular Chemistry

ROYAL SOCIETY OF CHEMISTRY

PAPER

View Article Online
View Journal | View Issue

Cite this: *Org. Biomol. Chem.*, 2024, **22**, 5965

Kinetic study of the reaction of thiophene-tocopherols with peroxyl radicals enlightenings the role of O•···S noncovalent interactions in H-atom transfer†

Andrea Baschieri, *[a] Zongxin Jin,[b] Riccardo Amorati, [b] Kristian Vasa,[c] Allegra Baroncelli,[c] Stefano Menichetti [c] and Caterina Viglianisi *[c]

Three new α-tocopherol thiophene derivatives were efficiently synthesized, characterized and used for the first time as chain-breaking antioxidants for the inhibition of the autoxidation of reference oxidizable substrates. The rate constant of the reaction with alkylperoxyl (ROO•) radicals and the stoichiometry of radical trapping (*n*) for the thiophene-tocopherol compounds were determined by measuring the oxygen consumption during the autoxidation of styrene or isopropylbenzene, using a differential pressure transducer. The measurement of the reaction with ROO• radicals in an apolar solvent at 30 °C showed inhibition rate constants (k_{inh}) in the order of 10^4 M^{-1} s^{-1}. To rationalise the kinetic results, the effect of the thiophene ring on the H-atom donation by O–H groups of the functionalized tocopherols was investigated by theoretical calculations. The importance of noncovalent interactions (including an unusual O•···S bond) for the stability of the conformers has been shown, and the O–H bond dissociation enthalpy (BDE (OH)) of these derivatives was determined. Finally, the photophysical properties of these new compounds were investigated to understand if the addition of thiophene groups changes the absorption or emission spectra of the tocopherol skeleton for their possible application as luminescent molecular probes.

Received 4th June 2024,
Accepted 26th June 2024

DOI: 10.1039/d4ob00944d

rsc.li/obc

Introduction

Phenols (ArOH) are probably the most important class of natural and synthetic antioxidants used for the protection of man-made items and living tissues from oxidation.[1–3] This ability depends on the transfer of an H atom from ArOH to, typically, peroxyl radicals (ROO•) with the formation of a relatively safe phenoxyl radical (ArO•). In living tissues, this radical can be reduced by various reductants (such as ascorbate, vitamin C) in a synergetic redox cycle.[4–7] Considering the key H• transfer process, the lower the bond dissociation energy (BDE) of the phenolic O–H, the higher the rate constant (k_{inh}) of the reaction with ROO•.[8–11] Thus, any stabilization of the starting phenol, for example, the involvement of the phenolic OH in a H bond,[12–15] will hamper the process, while any stabilization of Ar–O• will facilitate it. The transformation of Ar–OH into Ar–O• means transforming an electron-donating (ED) group into an electron-withdrawing (EW) group.[12] Therefore, ED groups on the aromatic ring strongly stabilize Ar–O•, facilitating the H• transfer.[12–15] Indeed, nature has selected tocopherols (TOH, Fig. 1), and in particular alpha-tocopherol (**α-TOH**, Fig. 1), the main component of vitamin E (Vit E), as the most potent lipophilic chain-breaking antioxidants for the protection of cell membranes and LDL from autoxidation.[16–18] Together with the three methyl groups, the ED *p*-alkoxy group plays a relevant role in stabilizing the α-TO• radical, but resonance stabilization requires a correct conformation, *i.e.*, one lone pair of the alkoxy oxygen should be parallel to the aromatic π orbitals. Actually, this situation takes place when the Ar–O–R dihedral angle is near to 0°, a situation that is facilitated by the alkoxy oxygen inserted in a benzo-fused six-membered ring or, even better, in a five-membered ring as in dihydrobenzo[*b*]-furanol (**DhyBF**) (Fig. 1).[12,15,19–21]

Accordingly, k_{inh} increases from 5,7,8-trimethyl-6-hydroxychromane (as in **α-TOH**) to dihydrobenzo[*b*]furanol (**DhyBF**) since the five-membered ring is almost coplanar with the aromatic ring.[12–15,19–21] Ingold and coworkers studied the stereoelectronic issues that make **α-TOH** the model for lipophilic

[a]*Institute for Organic Synthesis and Photoreactivity (ISOF), National Research Council of Italy (CNR), Via P. Gobetti 101, I-40129 Bologna, Italy. E-mail: andrea.baschieri@isof.cnr.it*
[b]*Department of Chemistry "G. Ciamician", University of Bologna, Via P. Gobetti 85, 40129 Bologna, Italy*
[c]*Department of Chemistry "Ugo Schiff" – DICUS, University of Florence, Via Della Lastruccia 3-13, I-50019 Sesto Fiorentino, Firenze, Italy. E-mail: caterina.viglianisi@unifi.it*

†Electronic supplementary information (ESI) available: NMR spectra of thieno compounds **8–13**. See DOI: https://doi.org/10.1039/d4ob00944d

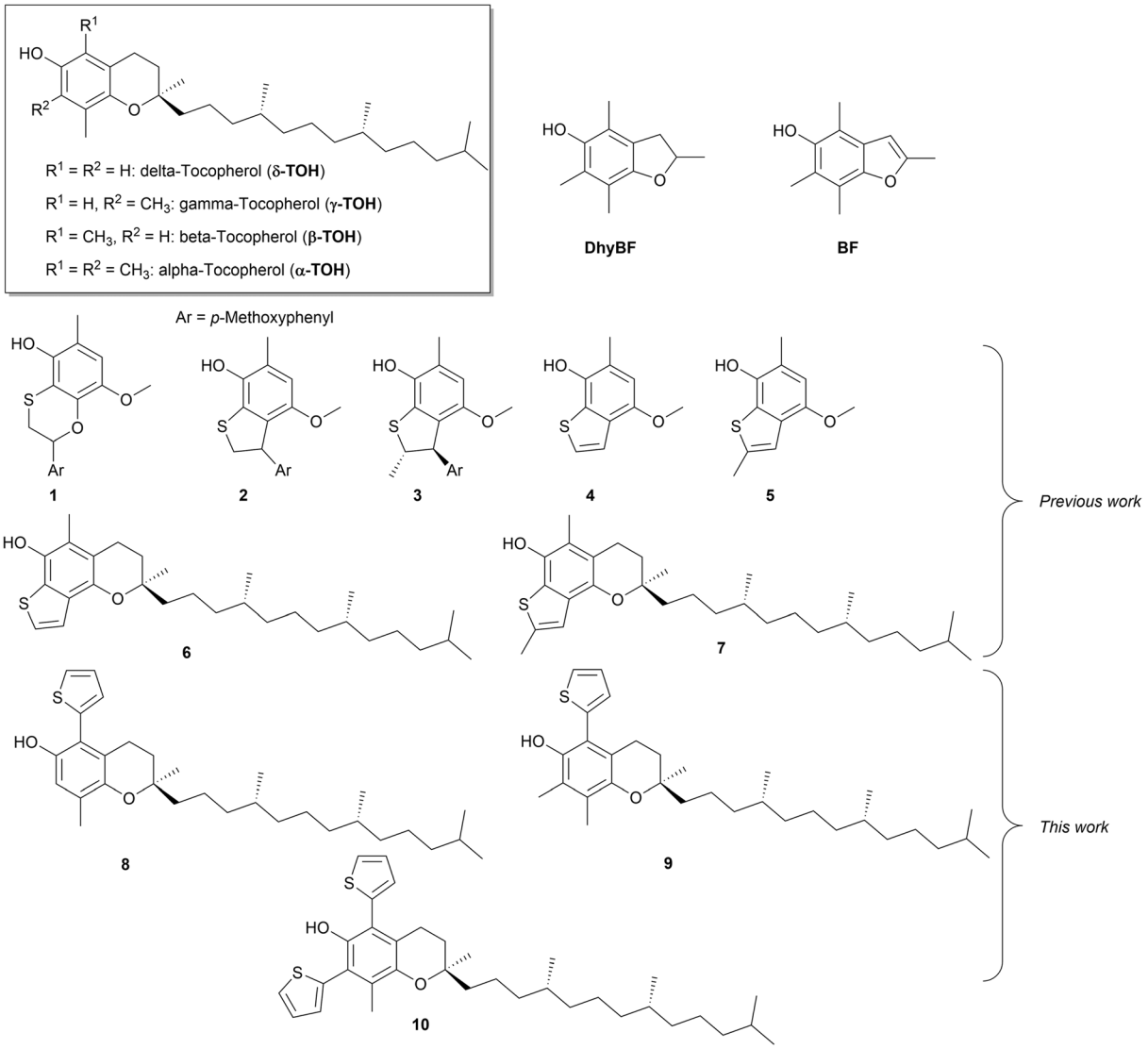

Fig. 1 Tocopherol derivatives and sulfur substituted phenolic antioxidants already present in the literature and thieno compounds **8–10** prepared in this study.

antioxidants and demonstrated that benzo[*b*]furanol (**BF**), despite its complete planarity, shows a significant decrease (roughly 10 times) of the H$^{\bullet}$ transfer ability.[22] This was explained by considering that aromatization reduced the ED ability of the endocyclic O atom.[22] The role played by the insertion of sulfur, and other chalcogens, in chain breaking and hydroperoxide quenching antioxidant activities of Ar–OH has been deeply investigated.[23–32] For example, sulfur-substituted phenolic antioxidants bearing the sulfur atom *ortho* to the phenolic OH and inserted in a benzoxathiine heterocyclic system (like compounds **1**, Fig. 1)[33] showed outstanding chain breaking antioxidant activities with k_{inh} equivalent to that of α-TOH (k_{inh} = 3.2 × 10^6 M^{-1} s^{-1}). This exceptional result is achieved thanks to the fact that sulfur is a poor acceptor of intramolecular H bonds, while maintaining its ED character and the ability to stabilize Ar–O$^{\bullet}$.[34–37] This also allowed us to propose a rationale for the post-translational cysteine–tyrosine linkage in the galactose oxidase (GAO) active site.[33]

Recently, exploiting a procedure based on an acid-mediated benzoxathiine–dihydrothiophene rearrangement, we efficiently prepared 7-hydroxydihydrobenzo[*b*]thiophenes like **2** and **3** (Fig. 1), showing, in turn, high k_{inh} (~1.4 × 10^6 M^{-1} s^{-1}).[38,39] When the benzoxathiine–dihydrothiophene rearrangement was carried out under harsher acidic conditions, dihydrobenzo[*b*]thiophenes **2** and **3** were transformed into benzo[*b*]thiophenes **4** and **5** (Scheme 1).[38,40]

Taking into consideration the previously reported evidence on the dihydrobenzo[*b*]furan *vs.* benzo[*b*]furan pair (**DhyBF** *vs.* **BF**),[22] we were very surprised to find that the measured k_{inh} of **4** or **5** was up to three times higher than that of the corresponding dihydro precursors **2** or **3**. Since a benzo[*b*]thiophene is, at least, as "aromatic" as a benzo[*b*]furan, a rationale for

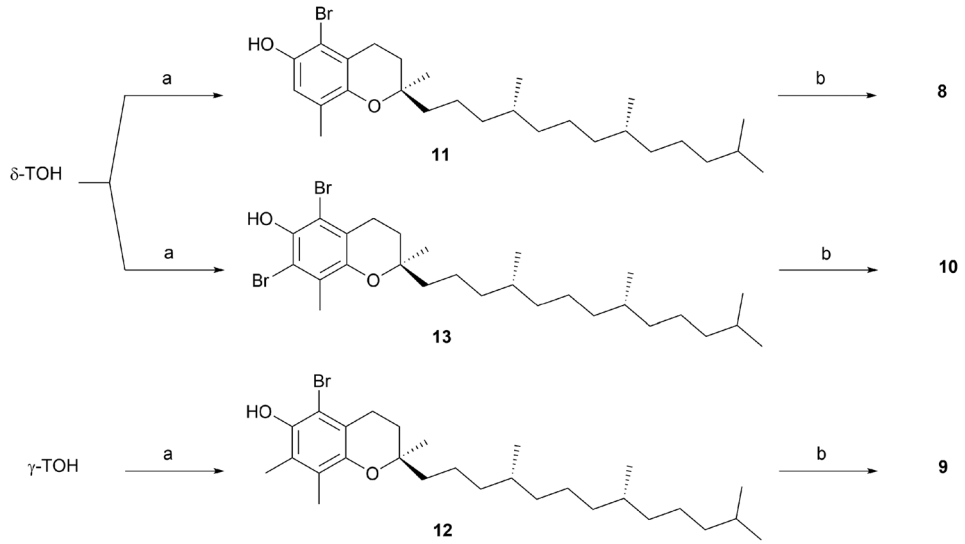

a: NBS (0.7 equivs for **11**, 1.0 equivs for **12**, 2.0 equivs for **13**), DCM dry, 0 °C, 2.5h, N_2 atm;
b: Acid 2-thienyl boronic (1.5 equivs for **8** and **9**, 3.0 equivs for **10**), THF dry, 2M Na_2CO_3 (2.0 equivs for **8** and **9**, 4.0 equivs for **10**), $Pd[P(t\text{-}Bu)_3]_2$ 10%mol for each carbon-bromine bond.

Scheme 1 Thieno tocopherols **8–10** synthesized in this study.

this result required envisaging some additional effect responsible for the extra stabilization of Ar–O$^{\bullet}$ involving the sulfur atom.[40] We suggested an intramolecular interaction between the electron-deficient area on the surface of the covalently bonded chalcogen (S or Se) and the negative surface of the O atom.[40] Indeed, the analysis of the electrostatic potential surfaces of the investigated compounds indicated, on the sulfur and selenium atoms, the presence of σ-holes[41,42] as two regions of positive potential along the outer sides of the carbon–chalcogen σ-bonds.

As a matter of fact, tocopheryl benzo[*b*]thiophenes **6** and **7**, designed and prepared to maximize the various effects due to the presence of the tocopherol skeleton and the sulfur atom, showed a higher chain breaking antioxidant activity, in terms of k_{inh}, than those previously reported (k_{inh} = 7.4 and 9.8 × 10^6 M^{-1} s^{-1} respectively) for sulfur containing phenolic antioxidants. Additionally, these compounds showed an interaction with the alpha-tocopheryl natural transporting enzyme pretty similar to the natural ligand α-TOH.[40]

In order to verify the 'chalcogen-bond effect' on Ar–O$^{\bullet}$ stabilization and possibly increase this effect making Ar–O$^{\bullet}$···S less structurally demanding than in **6** and **7**,[43–47] we designed compounds **8–10** (Fig. 1), where an extra bond is inserted between the phenolic oxygen and thiophene sulfur(s) while the skeleton of tocopherols is maintained.

The synthesis of **8–10**, the kinetics of the reaction with peroxyl radicals and theoretical calculations of the O–H bond dissociation enthalpy performed on these derivatives, and a rationale for the data acquired are discussed in this paper. In addition, the photophysical properties of these new compounds were investigated to understand if the addition of thiophene groups changes the fluorescence emission of the tocopherol skeleton for their possible application as molecular probes for antioxidant consumption during lipid peroxidation.[48] Tocopherols present absorption and emission peaks centered at approximately the same wavelength[49] and, even if several methods for the determination of tocopherols have been published,[50–54] their determination in a mixture is not feasible by the conventional fluorimetric technique.[55] It should be highlighted that spectroscopic methods show clear advantages over chromatographic techniques for the analysis of one or a few analytes, such as lower consumption of solvents, shorter analysis times, and lower cost of equipment.[55]

Results and discussion

Synthesis

The preparation of thieno derivatives **8–10** was achieved from the corresponding bromo-tocopherols in turn prepared by bromination of commercially available enantiopure δ- and γ-tocopherols as previously reported.[56,57] In particular, δ-tocopherol was mono- or bis-brominated with NBS to give derivatives **11** and **13** as reported in Scheme 1. Analogously, bromo-derivative **12** was prepared by reacting γ-tocopherol with NBS (Scheme 1). Although some procedures are available in the literature, these halogenations are very sensitive to the reaction conditions and an appropriate setup was necessary to isolate bromo-tocopherol in high purity and in reasonable yields (Fig. S1–S3†). With compounds **11–13** in hand, we carried out a Suzuki–Miyaura reaction with 2-thienyl boronic acid as a nucleophile, applying a slightly modified procedure reported to be effective for five-membered bromo-heteroaromatic compounds,[58] to obtain the expected thienyl-tocopherol compounds **8–10** (Scheme 1). Tocopherols **8–10** bearing 2-thienyl groups *ortho* to the OH groups were purified by flash

chromatography and fully characterized before conducting the antioxidant measurements (Fig. S4–S9†).

Autoxidation experiment

The rate constant of the reaction with alkylperoxyl (ROO$^\bullet$) radicals and the stoichiometry of radical trapping (n) for the title compounds were measured by studying the inhibition of the autoxidation of either styrene or cumene, two reference organic substrates whose autoxidation follows the kinetic scheme reported in eqn (1)–(6).[59]

$$\text{Initiator} \rightarrow \text{R}^\bullet \ (R_\text{i}) \quad (1)$$

$$\text{R}^\bullet + \text{O}_2 \rightarrow \text{ROO}^\bullet \quad (2)$$

$$\text{ROO}^\bullet + \text{RH} \rightarrow \text{ROOH} + \text{R}^\bullet \ (k_\text{p}) \quad (3)$$

$$\text{ROO}^\bullet + \text{ROO}^\bullet \rightarrow \text{non-radical products} \ (k_\text{t}) \quad (4)$$

$$\text{ROO}^\bullet + \text{AH} \rightarrow \text{ROOH} + \text{A}^\bullet \ (k_\text{inh}) \quad (5)$$

$$\text{ROO}^\bullet + \text{A}^\bullet \rightarrow \text{non-radical products} \quad (6)$$

$$-\text{d}[\text{O}_2]/\text{d}t = (k_\text{p}\ [\text{RH}]\ R_\text{i})/(n\ k_\text{inh}\ [\text{AH}]) + R_\text{i} \quad (7)$$

$$R_\text{i} = (n\ [\text{AH}]/\tau) \quad (8)$$

Here, RH is the substrate, AH is the antioxidant, and R$^\bullet$, ROO$^\bullet$ and A$^\bullet$ are alkyl, peroxyl and antioxidant-derived radicals, respectively. Based on reactions (5) and (6), the stoichiometry of radical trapping is ideally 2. In a typical autoxidation experiment, in the absence of antioxidants, a fast and linear O_2 consumption was observed; see for example traces "a" in Fig. 2. Instead, in the presence of antioxidants, the rate of O_2 consumption was reduced and an inhibition period (τ) in some cases could be detected. The rate of autoxidation of the substrate in the presence of the antioxidant AH obeys eqn (7), where k_p and $2k_t$ are, respectively, the rate constants of propagation and termination of the substrate and k_{inh} is the inhibition rate constant of the antioxidant (see the Experimental section for details).[59]

The stoichiometry can be obtained using eqn (8), where R_i is the effective rate of radical generation by AIBN and τ is the length of the inhibition time. R_i was measured by eqn (8) using a reference antioxidant, whose n is precisely known. The reactions were initiated by azo-bis(isobutyronitrile) (AIBN) at 30 °C, using chlorobenzene as the solvent, and were studied by monitoring the O_2 uptake by using a miniaturized differential pressure transducer.[60] Styrene was used because the kinetic parameters of its autoxidation closely resemble those of the natural unsaturated lipid linoleic acid, while cumene, being less oxidizable than styrene, allowed a better measure of the stoichiometric coefficient.[61] The results showed that the title compounds were weak inhibitors of the peroxidation of styrene (Fig. 2A), whereas they enabled strong inhibition of the autoxidation of cumene (Fig. 2B). The k_{inh} values that were obtained from these plots are reported in Table 1, together with the values, available in the literature, of α-tocopherol and β-tocopherol (for the structures, see Fig. 1).[59] The thiophene-tocopherols were much less reactive than their natural counterparts and presented the expected radical trapping stoichiometry of approximately 2.

Theoretical calculations

Puzzled by the slow reactivity of **8–10** with ROO$^\bullet$, the effect of the thiophene ring on the H-atom donation by the title phenols was investigated by theoretical calculations. As chlorobenzene phenols react through the H-atom transfer mechanism (HAT), we focused our attention on the O–H bond dissociation enthalpy (BDE).[62] First, we considered a model molecule constituted by a phenol and the thiophene ring linked at

Table 1 Rate constant for the reaction with ROO$^\bullet$ radicals (k_{inh}) and the stoichiometric coefficient (n) of the title compounds studied by the inhibited autoxidation of styrene or cumene in PhCl, initiated by AIBN at 30 °C

	k_{inh} (M^{-1} s^{-1}) cumene	k_{inh} (M^{-1} s^{-1}) styrene	n
8	$(1.1 \pm 0.2) \times 10^4$	$(7.0 \pm 0.1) \times 10^3$	1.6 ± 0.2
9	$(8.0 \pm 0.5) \times 10^4$	$(1.1 \pm 0.4) \times 10^5$	2.2 ± 0.2
10	$(3.2 \pm 0.3) \times 10^4$	$(1.8 \pm 0.2) \times 10^4$	2.1 ± 0.2
α-TOH [a]	3.2×10^6	—	2
β-TOH [a]	1.3×10^6	—	2

[a] From ref. 59.

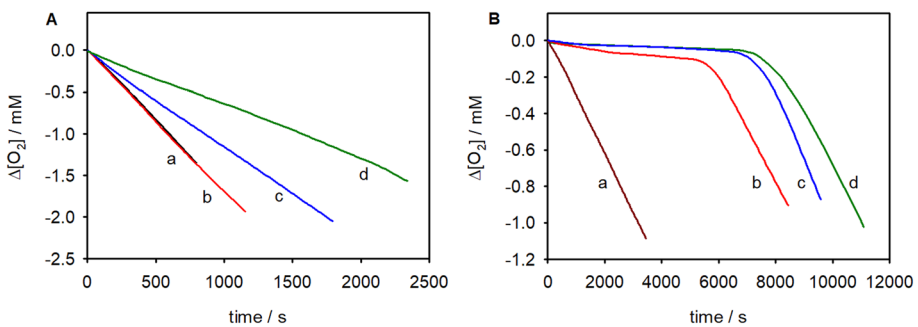

Fig. 2 Oxygen consumption rates at 30 °C observed during the autoxidation of styrene (panel A, 4.3 M) and cumene (panel B, 3.6 M) in chlorobenzene initiated by AIBN (0.025 M): in the absence of inhibitors (a, dashed line) or in the presence of 10 μM of the investigated antioxidants (b): **8**; (c): **10**; (d): **9**.

the *ortho* or *para* position in the phenolic aromatic ring. The stability of the conformers and the BDE was calculated at a high level of theory (CBS-QB3) in the gas phase (Scheme 2).[63] The thiophene substituent at the *para* position in the phenolic aromatic ring has a marked BDE-lowering effect (−4.6 kcal mol^{-1}), thanks to its ability to stabilize the phenoxyl radical by delocalization and electron donation. The possibility of delocalizing the unpaired electron is enabled by the planar arrangement of the two rings (Scheme 2a). When the thiophene ring is at the *ortho* position, it can interact with the phenolic OH in different ways, while steric repulsion also occurs. The preferred conformation is one where the two rings adopt a non-planar arrangement, with the OH bond pointing toward the thiophene aromatic ring (see Scheme 2b). This conformation, common for phenols having *ortho* aromatic substituents, can be explained in terms of a hydrogen bond between the OH group and the aromatic π electrons.[64,65] Interestingly, among the less stable conformations having the OH pointing away from the substituent, conformation **V** is more stable than **VI** by 0.8 kcal mol^{-1} (see Scheme 1), indicating attraction between O and S atoms. In addition, the S atom itself is a weak H-bond acceptor, as evident from the instability of conformation **III**.

After H-atom abstraction, the *ortho*-thiophene phenoxyl radical reported in Scheme 2c is formed. The phenoxyl radicals exist only in the planar conformation. The larger stability of the conformer having the S atom pointing toward the –O$^{\bullet}$ group suggests also in this case the presence of a non-covalent interaction between the S and O atoms. From this conformational analysis, it is possible to understand the contribution of the *ortho*-thiophene substituent to the BDE(OH). The most stable conformation of the *ortho*-thiophene phenol, having the S atom pointing away from the OH group, has a BDE(OH) of 84.8 kcal mol^{-1} (see Scheme 2d). The corresponding substituent effect of −2.3 kcal mol^{-1} is smaller than that of the thiophene at the *para* position, because of the stabilization of the phenol by an H bond between the OH and the thiophene ring. The slightly less stable conformation (by +0.4 kcal mol^{-1}) of the *ortho*-thiophene phenol has a BDE(OH) of 83.1 kcal mol^{-1} and a substituent effect of −4.0 kcal mol^{-1}, mainly due to the effect of the O$^{\bullet}$···S interaction in the phenoxyl radical. Herein, it can be noticed that a major conformational change in the dihedral angle between the two rings occurs when transitioning from the phenol to the radical, suggesting that the BDE(OH) may not reflect the radical stabilization in the transition state

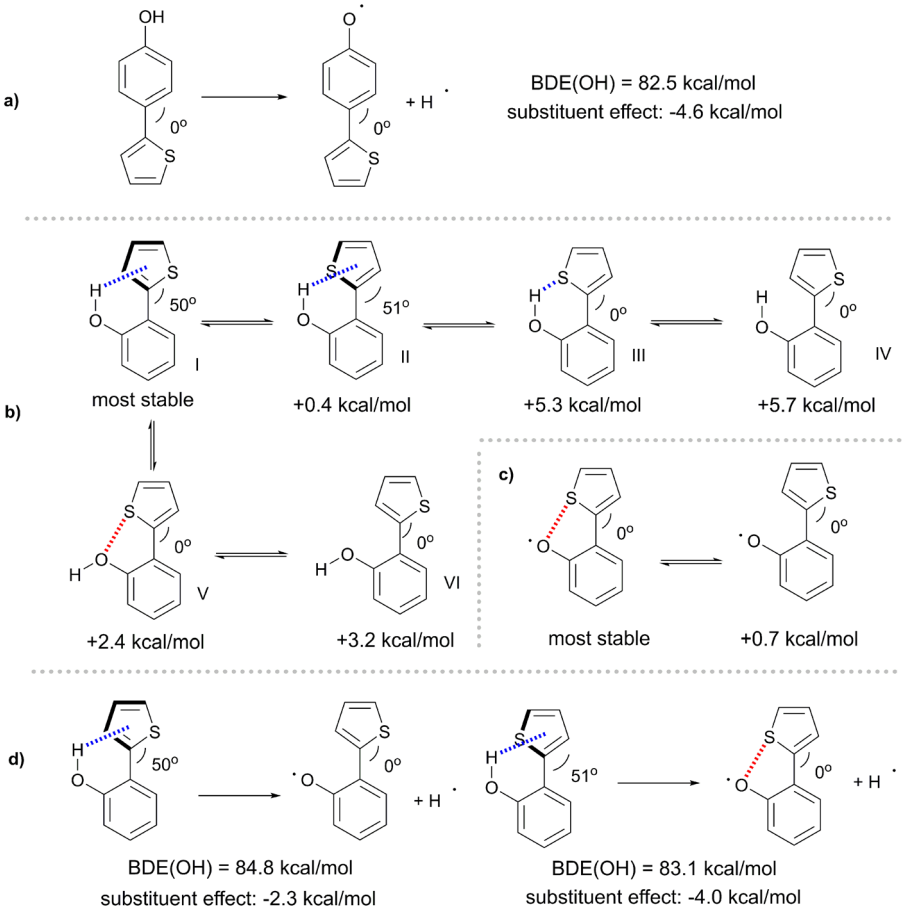

Scheme 2 Calculated (CBS-QB3) BDE(OH) and conformational stability for the phenol-thiophene model. (a) Optimized conformation and BDE(OH) for the *para* isomer; (b) conformational stability of the *ortho* isomer; (c) conformational stability of the phenoxyl radicals; (d) BDE(OH) of the most stable conformations of the phenol.

of H-atom abstraction, as previously reported by us for *ortho* substituted phenols.[64,66]

Having shown the importance of conformation to determine the BDE(OH), the complete structure of the title compounds was then considered, and calculations were performed at an intermediate level of theory (B3LYP/6-31+g(d,p)) that could represent a trade-off between accuracy and computational cost, and that was successfully used to describe H-bond equilibria and conformations in phenols.[64–66] The results, reported in Scheme 3, show that the structure of tocopherol introduces steric repulsion that causes the thiophene to adopt a nearly perpendicular conformation in the parent phenols (dihedral angles vary from 76° to 86°) and a non-planar conformation in the radicals. The latter effect is expected to drastically reduce the stabilization of the radical by the thiophene ring, causing an increase of the BDE (OH). Moreover, when comparing **9** with **10**, which have equal BDE(OH) values, the higher reactivity of **9** than that of **10** is due to the smaller steric effect of CH_3 compared to the thiophene ring.[26] Overall, the calculated BDE(OH) values of the title compounds reported in Scheme 3c provide evidence for their low reactivity toward ROO$^{\bullet}$ radicals compared to α and β-tocopherols.

Photophysical characterization

The photophysical properties of compounds **8–10** were investigated at room temperature in solution and at 77 K in a rigid matrix and compared to those of 2,2,5,7,8-pentamethyl-6-chromanol (PMHC), a synthetic analogue of α-tocopherol. PMHC has a simple structure, similar to that of our compounds, but without the presence of thiophene units and with a methyl group at the 2-position instead of the long alkyl chain, present in all tocopherol derivatives. The room temperature absorption and fluorescence emission spectra of compounds **8–10** and PMHC in dichloromethane solution are reported in Fig. 3, together with phosphorescence spectra in the rigid matrix at 77 K (Fig. 3B).

The absorption spectra of **8** and **9** are almost superimposable, suggesting that the insertion of one methyl group has negligible influence on both the energy and the profile of the lowest-energy absorption band of these compounds. In contrast, the addition of a second thiophene unit causes a red shift of the lowest-energy absorption band (*i.e.*, from 308 for **8** and **9** to 316 nm for **10**, approximately). This effect is confirmed also considering the absorption spectrum of the reference compound PMHC. The absence of thiophene groups makes this compound the one with less intense absorption spectra and a blue-shifted absorption maximum.

Despite the differences in their absorption profiles, these compounds present very similar fluorescence spectra, with an unstructured band centered at approx. 385 nm. Only **10** has an emission maximum slightly red-shifted by 10 nm. Even fluorescence quantum yields are virtually identical for all the compounds (*i.e.*, around 0.2% and 0.4% in dichloromethane solu-

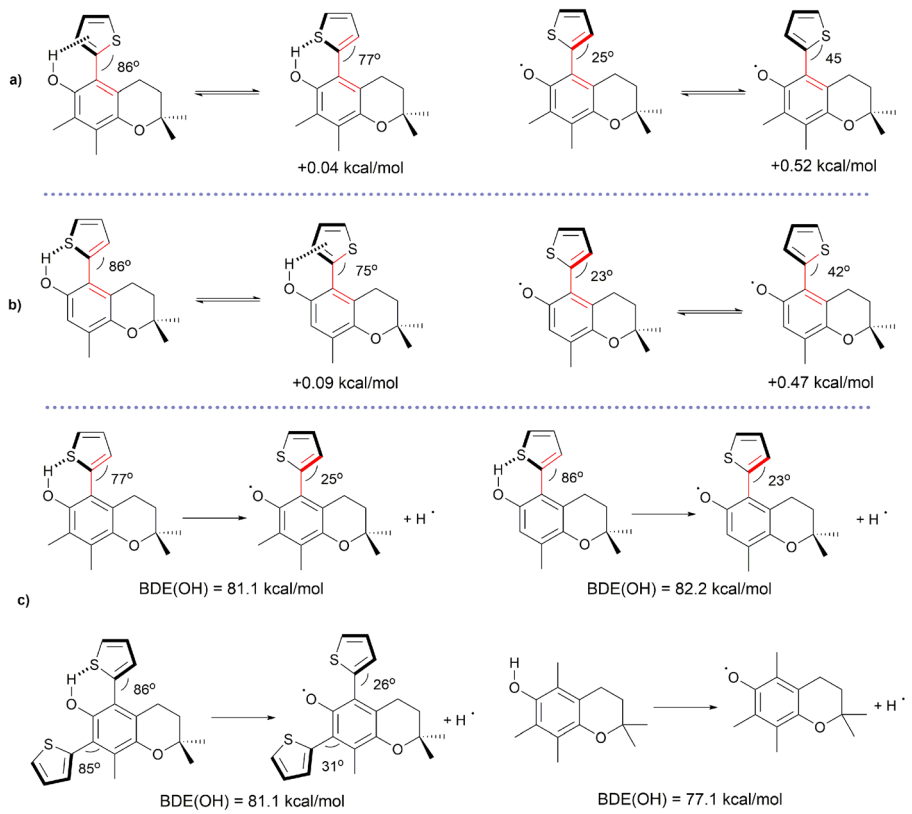

Scheme 3 Calculated (B3LYP/6-31+g(d,p)) BDE(OH) and conformational stability for the tocopherol-thiophenes. (a and b) Most stable conformations of **9**, **10** and their phenoxyl radicals; (c) BDE(OH) of the most stable conformations of **8**, **9** and **10**.

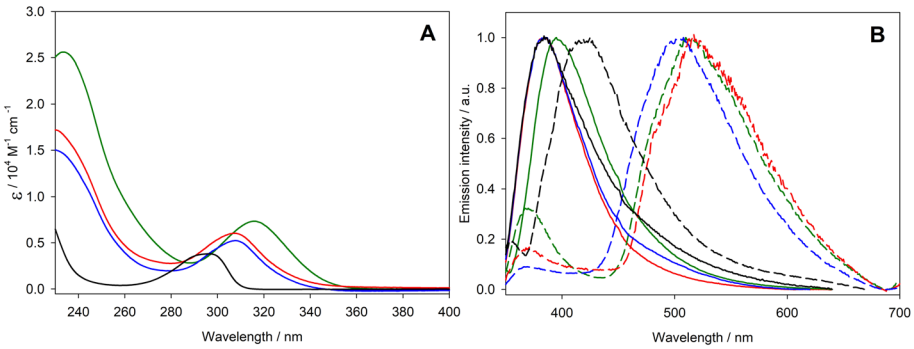

Fig. 3 Panel A: Absorption spectra of antioxidants **8–10** in room-temperature dichloromethane solution. PMHC (black), **10** (green), **8** (red) and **9** (blue). Panel B: Normalized emission spectra of complexes **8–10** in dichloromethane solutions at 298 K (solid) and in 2-methyl tetrahydrofuran glass at 77 K (dashed). Sample concentration: ≈20 μM. PMHC (black), **10** (green), **8** (red) and **9** (blue).

Table 2 Luminescence properties and photophysical parameters of compounds **8–10** and in solution

	DCM solution (298 K)						2Me-THF glass (77 K)			
		Fluorescence					Fluorescence		Phosphorescence	
	Absorption λ_{abs} [nm]	λ_{em} [a] [nm]	PLQY[a] [%]	τ [b] [ns]	k_r [c] [10^6 s^{-1}]	k_{nr} [d] [10^8 s^{-1}]	λ_{em} [a] [nm]	τ [b] [ns]	λ_{em} [a] [nm]	τ [b] [ms]
8	308	385	0.4	4.3	0.98	2.32	371	5.4	516	45
9	308	385	0.2	1.2	1.40	9.08	370	2.9	508	41
10	316	395	0.3	2.2	1.42	4.53	370	3.1	512	45
PMHC	296	384	0.2	6.1	0.45	1.63	356	10.1	418	1602

[a] λ_{exc} = 316 nm for **10**, 308 nm for **8** and **9**, and 295 nm for **PMHC**. [b] λ_{exc} = 331 nm. [c] Radiative constant: k_r = PLQY/τ. [d] Non-radiative constant: k_{nr} = $1/\tau - k_r$.

tions), despite the excited-state lifetime ranging from 2 ns to 6 ns (see Table 2).

The 77 K emission spectra of compounds **8–10** in 2-methyl tetrahydrofuran frozen glass show the presence of fluorescence and phosphorescence (Fig. 3B). The fluorescence spectra at 77 K exhibit just a small band around 370 nm, comparable with the one at room temperature, even if much less intense. The phosphorescence spectrum of derivatives with one or two thiophene units shows an unstructured band centered at approximately 510 nm. To confirm that it is a phosphorescent emission, we recorded the triplet lifetimes, which reach approximately 45 ms. This value is 6 orders of magnitude higher than the lifetime recorded at room temperature and consistent with those of phosphorescent organic compounds at 77 K.[67] We also studied the lifetime of samples **8–10** in a poly(methyl methacrylate) matrix at a sample concentration of 1% by weight, but, unfortunately, in the solid state, phosphorescence is not maintained. This property at 77 K is also observed for the reference compound PMHC, but with a blue-shifted emission maximum of about 90 nm (*i.e.*, 418 for PMHC and 510 for **8–10**) and with triplet lifetimes, which reach approximately 1.6 s. These results indicate that the thiophene moieties play a fundamental role in diversifying the absorption spectrum of these new compounds compared to the reference compound PMCH, while the emission properties at room temperature remain almost unchanged.

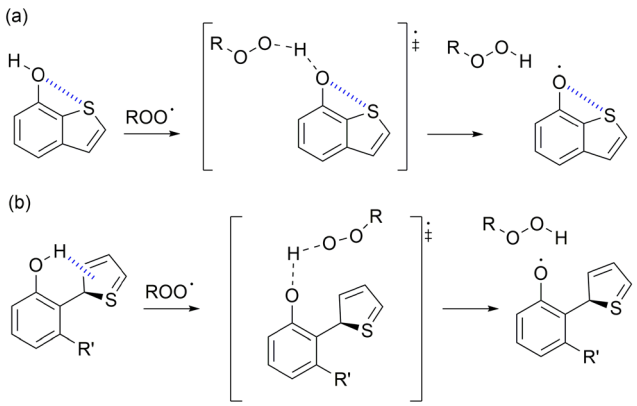

Scheme 4 Importance of non-covalent O•···S interaction for the stabilization of the phenoxyl radical in previously reported compounds **6** and **7** and in tocopherol-thiophene derivatives **8–10**.

Conclusions

In this work, we determined the rate constant of the reaction with ROO• radicals of three α-tocopherol derivatives with an *ortho*-thiophene substituent. Differently from what was previously found with benzo[*b*]thiophenes **6** and **7**, in which the thiophene moiety was fused to the phenol ring and led to a significant improvement in the reactivity with ROO• radicals,

herein the *ortho*-thiophene substituent decreased the chain-breaking antioxidant activity. The inhibition rate constants (k_{inh}) are in the order of 10^4 M^{-1} s^{-1}, which is a value typical of medium-strength antioxidants like 2,6-di-*tert*-butyl-4-methylphenol (BHT),[3] but is smaller than those of the natural reference compounds α-tocopherol and β-tocopherol.

Previous studies showed that the activity of benzo[*b*]thiophenes had to be ascribed to a favorable O•···S non-covalent interaction in the phenoxyl radical of **6** and **7** (Scheme 4). Moreover, because of the rigidity of the molecular scaffold of **6** and **7**, this interaction was also effective in the incipient radical formed during the transition state. However, from the present results, it appears that such an O•···S interaction is not present in tocopherol-thiophene derivatives **8–10**, because the steric repulsion between the tocopherol skeleton and the thiophene ring precluded the formation of a planar conformation necessary for the stabilization of the transition state of H-atom abstraction by ROO• radicals. The reactivity of **8–10** was further diminished by an H-bond interaction by the OH and the thiophene groups in the parent phenols.

As a result, these findings offer a fresh perspective on the complex effects of non-covalent interactions on the transfer of H atoms from phenols to radicals. Based on the ability of relatively inexpensive DFT calculations to predict the behaviour of these systems demonstrated herein, future studies will be aimed at designing novel derivatives with a more favourable O•···S interaction, for example by forcing the thiophene in a planar conformation. Moreover, the role of heavier chalcogens (*i.e.*, selenium) could be explored.

Moreover, all the three new α-tocopherol thiophene derivatives showed similar luminescence properties. Compound **10** (having two thiophene groups) displayed a different absorption profile with a red shift of the lowest-energy absorption band (*i.e.*, from 308 nm for **8** and **9** to 316 nm for **10**, approximately), while the emission properties at room temperature of compounds **8–10** remained almost unchanged and are comparable with those of the reference PMHC.

These results provide a rational basis for the development of novel and possibly pharmacologically active antioxidants with interesting luminescence properties and potential new applications.

Experimental

Materials and methods

Solvents of the highest purity grade were used as received. Cumene and styrene were twice percolated on an alumina and silica gel column before use. AIBN was recrystallized from methanol. δ and γ-tocopherols were commercially available.

Synthetic procedures

(*R*)-5-Bromo-2,8-dimethyl-2-((4*R*,8*R*)-4,8,12 trimethyltridecyl) chroman-6-ol (11). In a reaction flask, δ-tocopherol (85 mg, 0.21 mmol) was solubilized in 2 mL of DCM. The solution was cooled to 0 °C and NBS (30 mg, 0.17 mmol) was added. The reaction mixture was kept at 0 °C under a N_2 atmosphere monitored by TLC, using Ep/AcOEt 10/1 as the eluent. Once the bromination was complete (2.5 h), a solution of Na_2SO_3 (106 mg, 0.84 mmol) in 2 ml of H_2O was added. The organic phase was collected, while the aqueous phase was washed with DCM (4 × 10 mL). The organic phases were then reunited, washed with brine (1 × 20 mL), and dried over anhydrous Na_2SO_4 and the solvent was removed under reduced pressure. The crude product was purified by silica gel flash column chromatography using Ep/AcOEt 10/1 as the eluent to obtain (*R*)-5-bromo-2,8-dimethyl-2-((4*R*,8*R*)-4,8,12-trimethyltridecyl) chroman-6-ol (**11**) (53 mg, 53% yield) as a colorless oil. ^{1}H NMR (200 MHz, $CDCl_3$) δ 6.73 (1H, s), 5.05 (1H, s), 2.72–2.65 (2H, t), 2.11 (3H, s), 1.84–1.75 (2H, m).[56,57]

(*R*)-5,7-Dibromo-2,8-dimethyl-2-((4*R*,8*R*)-4,8,12-trimethyltridecyl) chroman-6-ol (13). In a reaction flask, δ-tocopherol (130 mg, 0.32 mmol) was solubilized in 3 mL of dry DCM. The solution was cooled to 0 °C and NBS (114 mg, 0.64 mmol) was added. The reaction mixture was kept at 0 °C under a N_2 atmosphere monitored by TLC, using Ep/AcOEt 10/1 as the eluent. Once the bromination was complete (2.5 h), a solution of Na_2SO_3 (114 mg, 0.90 mmol) in 3 ml of H_2O was added. The organic phase was collected, while the aqueous phase was washed with DCM (4 × 15 mL). The organic phases were then reunited, washed with brine (2 × 20 mL), and dried over anhydrous Na_2SO_4 and the solvent was removed under reduced pressure. The crude product was purified by silica gel flash column chromatography using Ep/AcOEt 30/1 as the eluent to obtain (*R*)-5,7-dibromo-2,8-dimethyl-2-((4*R*,8*R*)-4,8,12-trimethyltridecyl)chroman-6-ol (**13**) (55 mg, 31% yield) as a colorless oil. ^{1}H NMR (200 MHz, CDCl3) δ 5.54 (1H, s), 2.71–2.65 (2H, t), 2.25 (3H, s), 1.79–1.49 (2H, m).[56,57]

(*R*)-5-Bromo-2,7,8-trimethyl-2-((4*R*,8*R*)-4,8,12-trimethyltridecyl) chroman-6-ol (12). In a reaction flask, γ-tocopherol (45 mg, 0.11 mmol) was solubilized in 1 mL of dry DCM. The solution was cooled to 0 °C and NBS (19 mg, 0.11 mmol) was added. The reaction mixture was kept at 0 °C in the dark and under a N_2 atmosphere monitored by TLC, using Ep/AcOEt 10/1 as the eluent. Once the bromination was complete (3.5 h), the solvent was directly removed under reduced pressure. The crude product was purified by silica gel flash column chromatography using Ep/Et_2O 10/1 as the eluent to obtain (*R*)-5-bromo-2,7,8-trimethyl-2-((4*R*,8*R*)-4,8,12-trimethyltridecyl)chroman-6-ol (**12**) (53 mg, 88% yield) as a pale yellow oil. ^{1}H NMR (200 MHz, $CDCl_3$) δ 5.20 (1H, s), 2.71–2.64 (2H, t), 2.22 (3H, s), 2.09 (3H, s), 1.83–1.75 (2H, m), 1.60–1.09 (22H, m), 0.87–0.83 (15H, m).[56,57]

(*R*)-2,8-Dimethyl-5-(thiophen-2-yl)-2-((4*R*,8*R*)-4,8,12-trimethyltridecyl)chroman-6-ol (8). In dry THF (2 mL), a mixture of bromo derivative **11** (68 mg, 0.14 mmol), thiophen-2-yl-boronic acid (23 mg, 0.18 mmol), $Pd(P(tBu)_3)_2$ (7 mg, 0.01 mmol) and 141 μL of a 2 M aqueous solution of K_2CO_3 was kept at 80 °C for 24 h under a N_2 atmosphere. The solution was cooled at room temperature, quenched with saturated NH_4Cl (30 mL) and separated, and the aqueous phase was washed with hexane (3 × 20 mL). The collected organic phase was dried over

anhydrous Na_2SO_4, filtered, and dried under reduced pressure. The crude product was purified using a silica gel chromatography column and $CHCl_3$ as the eluent to obtain (*R*)-2,8-dimethyl-5-(thiophen-2-yl)-2-((4R,8*R*)-4,8,12-trimethyltridecyl) chroman-6-ol (**8**) (12 mg, 18% yield) as a colorless oil. ^{1}H NMR (200 MHz, $CDCl_3$) δ 7.90–7.47 (1H, m), 7.19–7.15 (1H, m), 7.01–6.98 (1H, m), 6.68 (1H, s), 4.67 (1H, s), 2.53–2.45 (2H, t), 2.18 (3H, s), 1.71–1.63 (2H, m), 1.55–0.98 (21H, m), 0.88–0.82 (15H, m). ^{13}C NMR (100 MHz, $CDCl_3$) δ 146.6, 145.9, 135.9, 128.8, 128.7, 127.9, 127.7, 120.7, 116.6, 115.2, 75.1, 40.1, 39.5, 37.6, 37.6, 37.5, 33.0, 32.9, 31.4, 28.1, 25.0, 24.6, 24.2, 22.9, 22.8, 21.7, 21.1, 19.9, 19.8, 16.4. FTIR ν 3691, 3535, 2924, 2866, 1469, 1428, 1376, 1260, 1214, 1158, 857, 698 cm^{-1}. ESI-MS: negative ion mode: *m*/*z* 483 $[M - H]^-$. Elemental analysis calcd for $C_{31}H_{48}O_2S$: C, 76.81; H, 9.98; found: C, 76.66; H, 10.07.

(*R*)-2,8-Dimethyl-5,7-di(thiophen-2-yl)-2-((4*R*,8*R*)-4,8,12-trimethyltridecyl)chroman-6-ol (10). In dry de-oxygenated THF (2 mL), a mixture of di-bromo derivative **13** (74 mg, 0.13 mmol), thiophen-2-yl-boronic acid (44 mg, 0.35 mmol), $Pd(P(tBu)_3)_2$ (15 mg, 0.03 mmol) and 275 μL of a 2 M aqueous solution of K_2CO_3 was kept at 80 °C for 4 h and at 65 °C for an additional 22 h under a N_2 atmosphere. The solution was cooled at room temperature, quenched with saturated NH_4Cl (30 mL) and separated and the aqueous phase was washed with hexane (3 × 20 mL). The collected organic phase was dried over anhydrous Na_2SO_4, filtered, and dried under reduced pressure. The crude product was purified using a silica gel chromatography column and Ep/AcOEt 30/1 as the eluent to obtain (*R*)-2,8-dimethyl-5,7-di(thiophen-2-yl)-2-((4*R*,8*R*)-4,8,12-trimethyltridecyl)chroman-6-ol (**10**) (26 mg, 35% yield) as a colorless oil. ^{1}H NMR (200 MHz, $CDCl_3$) δ 7.46–7.43 (2H, m), 7.17–7.12 (2H, m), 7.03–6.99 (2H, m), 4.87 (1H, s), 2.60–2.54 (2H, t), 2.07 (3H, s), 1.77–1.64 (3H, m), 1.54–1.05 (20H, m), 0.88–0.83 (15H, m). ^{13}C NMR (100 MHz, $CDCl_3$) δ 145.8, 145.4, 136.9, 136.4, 128.4, 128.3, 128.2, 127.5, 127.4, 127.0, 126.9, 122.0, 119.6, 116.9, 75.5, 40.3, 39.5, 37.6, 37.5, 33.0, 32.9, 31.4, 28.1, 25.0, 24.6, 24.3, 22.9, 22.8, 21.9, 21.2, 19.9, 19.9, 13.9. ESI-MS: negative ion mode: *m*/*z* 565.15 $[M - H]^-$. Elemental analysis calcd for $C_{35}H_{50}O_2S_2$: C, 74.15; H, 8.89; found: C, 74.31; H, 8.69.

(*R*)-2,7,8-Trimethyl-5-(thiophen-2-yl)-2-((4*R*,8*R*)-4,8,12-trimethyltridecyl)chroman-6-ol (9). In dry de-oxygenated THF (2 mL), a mixture of bromo derivative **12** (51 mg, 0.10 mmol), thiophen-2-yl-boronic acid (17 mg, 0.13 mmol), $Pd(P(tBu)_3)_2$ (7 mg, 0.01 mmol) and 103 μL of a 2 M aqueous solution of K_2CO_3 was kept at 80 °C for 24 h under a N_2 atmosphere. The solution was cooled at room temperature, quenched with saturated NH_4Cl (30 mL) and separated, and the aqueous phase was washed with hexane (3 × 20 mL). The collected organic phase was dried over anhydrous Na_2SO_4, filtered, and dried under reduced pressure. The crude product was purified using a silica gel chromatography column and Ep/AcOEt 10/1 as the eluent to obtain (*R*)-2,7,8-trimethyl-5-(thiophen-2-yl)-2-((4*R*,8*R*)-4,8,12-trimethyltridecyl)chroman-6-ol (**9**) (17 mg, 33% yield) as a colorless oil. ^{1}H NMR (400 MHz, $CDCl_3$) δ 7.50–7.48 (1H, dd), 7.19–7.17 (1H, m), 7.01–6.99 (1H, m), 4.80 (1H, s), 2.48–2.45 (2H, t), 2.20 (3H, s), 2.17 (3H, s), 1.73–1.62 (2H, m), 1.57–1.05 (22H, m), 0.88–0.84 (14H, m). ^{13}C NMR (100 MHz, $CDCl_3$) δ 145.7, 145.5, 136.5, 129.0, 128.3, 128.1, 127.5, 122.1, 118.3, 116.2, 73.5, 40.5, 39.8, 37.9, 37.9, 37.8, 33.3, 33.2, 31.8, 30.2, 28.5, 25.3, 24.9, 24.9, 23.2, 23.1, 21.9, 21.5, 20.2, 20.1, 12.7, 12.5. FTIR ν 3690, 3537, 2922, 2867, 1469, 1430, 1376, 1260, 1214, 1158 cm^{-1}. ESI-MS: negative ion mode: *m*/*z* 497 $[M - H]^-$. Elemental analysis calcd for $C_{32}H_{50}O_2S$: C, 77.05; H, 10.10; found: C, 76.88; H, 10.00.

Autoxidation experiments

Autoxidation experiments were performed in a two-channel oxygen uptake apparatus, based on a Validyne DP 15 differential pressure transducer built in our laboratory.[68] In a typical experiment, an air-saturated solution of either styrene or cumene containing AIBN was equilibrated with an identical reference solution containing excess 2,2,5,7,8-pentamethyl-6-hydroxychromane (PMHC) (25 mM). After equilibration, and when a constant O_2 consumption was reached, a concentrated solution of the antioxidant (final concentration = 5–10 μM) was injected in the sample flask. The oxygen consumption in the sample was measured after calibration of the apparatus from the differential pressure recorded with time between the two channels. The initiation rates, R_i, were determined for each condition in preliminary experiments by the inhibitor method using PMHC as a reference antioxidant: $R_i = 2[PMHC]/\tau$, where τ is the length of the induction period.

The inhibition rate constants were determined by using the kinetic equations previously reported[69] from the known k_p = 41 M^{-1} s^{-1} of styrene and k_p = 0.32 M^{-1} s^{-1} of cumene.

Theoretical calculations

The geometry optimization and frequency calculations of the thiophene-phenol model were performed in the gas phase at the CBS-QB3 level and the geometry optimization and frequency calculations of the complete structures were performed in the gas phase at the B3LYP/6-31+g(d,p) level using Gaussian 16. Stationary points were confirmed by checking the absence of imaginary frequencies. BDE values were obtained from the sum of electronic and thermal enthalpies by using the isodesmic approach, which consists of calculating the ΔBDE(OH) between the investigated compounds and PMHC and by adding this value to the known experimental BDE(OH) of PMHC in benzene (77.1 kcal mol^{-1}).[70,71] We have previously shown that gas phase calculations provide results in good agreement with experimental results in PhCl.[63–65] The free energy changes for the H-bond equilibria were calculated in the gas phase from the differences between the free energies of the products and those of the reactants.

Photophysical measurements

The spectroscopic investigations were carried out in spectrofluorimetric-grade solvents (*i.e.*, dichloromethane and 2-methyl tetrahydrofuran). The absorption spectra were recorded with a PerkinElmer Lambda 950 spectrophotometer. For the photoluminescence experiments, the sample solutions

were placed in fluorimetric Suprasil quartz cuvettes (10.00 mm). The uncorrected emission spectra were obtained with an Edinburgh Instruments FLS920 spectrometer equipped with a Peltier-cooled Hamamatsu R928 photomultiplier tube (spectral window: 185–850 nm). An Osram XBO xenon arc lamp (450 W) was used as the excitation light source. The corrected spectra were acquired by means of a calibration curve, obtained using an Ocean Optics deuterium–halogen calibrated lamp (DH-3plus-CAL-EXT). Phosphorescence spectra and the associated long-lived decay signals were acquired using the same Edinburgh FLS920 spectrometer using a μF920H flash lamp as the excitation source.

The photoluminescence quantum yields (PLQYs) in solution were obtained from the corrected spectra on a wavelength scale (nm) and measured according to the approach described by Demas and Crosby,[72] using an air-equilibrated water solution of quinine sulfate in 1 N H_2SO_4 as the reference (PLQY = 0.546).[73] The emission lifetimes (τ) were measured through the time-correlated single photon counting (TCSPC) technique using a HORIBA Jobin Yvon IBH FluoroHub controlling a spectrometer equipped with a pulsed NanoLED (λ_{exc} = 331 nm) as the excitation source and a red-sensitive Hamamatsu R-3237-01 PMT (185–850 nm) as the detector. The analysis of the luminescence decay profiles was accomplished using the DAS6 Decay Analysis Software provided by the manufacturer, and the quality of the fit was assessed with the χ^2 value close to unity and with the residuals regularly distributed along the time axis. To record the 77 K luminescence spectra, samples were put in quartz tubes (2 mm inner diameter) and inserted into a special quartz Dewar flask filled with liquid nitrogen. Poly(methyl methacrylate) (PMMA) films containing 1% (w/w) of the compound were obtained by drop-casting, and the thickness of the films was not controlled. Experimental uncertainties are estimated to be ±8% for τ determinations, ±10% for PLQYs, and ±2 and ±5 nm for absorption and emission.

Author contributions

A. B., R. A., S. M. and C. V. supervised and coordinated the project. R. A., C. V. and S. M. were responsible for funding acquisition. K. V. and A. B. synthesized the compounds and, together with C. V., were responsible for their structural characterization. The antioxidant experiments and DFT calculations were carried out by Z. J. and R. A. while the photophysical studies were carried out by A. B. All the authors reviewed, edited, and approved the final version of the manuscript.

Data availability

The data supporting this article have been included as part of the ESI.†

Conflicts of interest

There are no conflicts to declare.

Acknowledgements

Z. J. acknowledges the Chinese Service Center for Scholarly Exchange [202209120002]. We acknowledge the CINECA award under the ISCRA initiative, for the availability of high performance computing resources and support. Italian MIUR through Progetto Dipartimenti di Eccellenza 2023–2027 (DICUS 2.0) to the Department of Chemistry "Ugo Schiff" of the University of Florence is acknowledged. R. A. acknowledges funding by the European Union – NextGenerationEU under the National Recovery and Resilience Plan (PNRR) – Mission 4 Education and research – Component 2 From research to business – Investment 1.1 Notice Prin 2022 – DD N. 104 del 2/2/2022, from PRIN20227XZKBY – Superoxide responsive redox-active systems and nano smart materials to target ferroptosis – FEROX – CUP J53D23008550006.

References

1 K. U. Ingold, *Chem. Rev.*, 2002, **61**, 563–589.
2 M. de Fátima Poças and T. Hogg, *Trends Food Sci. Technol.*, 2007, **18**, 219–230.
3 K. U. Ingold and D. A. Pratt, *Chem. Rev.*, 2014, **114**, 9022–9046.
4 R. Amorati, F. Ferroni, M. Lucarini, G. F. Pedulli and L. Valgimigli, *J. Org. Chem.*, 2002, **67**, 9295–9303.
5 M. Eggersdorfer, D. Laudert, U. Letinois, T. McClymont, J. Medlock, T. Netscher and W. Bonrath, *Angew. Chem., Int. Ed.*, 2012, **51**, 12960–12990.
6 C. Golumbic and H. A. Mattill, *J. Am. Chem. Soc.*, 2002, **63**, 1279–1280.
7 B. Zhou, L. M. Wu, L. Yang and Z. L. Liu, *Free Radicals Biol. Med.*, 2005, **38**, 78–84.
8 J. S. Wright, D. J. Carpenter, D. J. McKay and K. U. Ingold, *J. Am. Chem. Soc.*, 1997, **119**, 4245–4252.
9 G. W. Burton and K. U. Ingold, *J. Am. Chem. Soc.*, 2002, **103**, 6472–6477.
10 J. S. Wright, E. R. Johnson and G. A. DiLabio, *J. Am. Chem. Soc.*, 2001, **123**, 1173–1183.
11 M. Lucarini and G. F. Pedulli, *Chem. Soc. Rev.*, 2010, **39**, 2106–2119.
12 L. R. C. Barclay, C. E. Edwards and M. R. Vinqvist, *J. Am. Chem. Soc.*, 1999, **121**, 6226–6231.
13 M. Lucarini, V. Mugnaini, G. F. Pedulli and M. Guerra, *J. Am. Chem. Soc.*, 2003, **125**, 8318–8329.
14 G. Litwinienko and K. U. Ingold, *Acc. Chem. Res.*, 2007, **40**, 222–230.
15 M. C. Foti, R. Amorati, G. F. Pedulli, C. Daquino, D. A. Pratt and K. U. Ingold, *J. Org. Chem.*, 2010, **75**, 4434–4440.
16 R. Brigelius-Flohé and M. G. Traber, *FASEB J.*, 1999, **13**, 1145–1155.
17 M. G. Traber and J. Atkinson, *Free Radicals Biol. Med.*, 2007, **43**, 4–15.
18 A. Azzi, *Free Radicals Biol. Med.*, 2007, **43**, 16–21.
19 G. W. Burton, Y. Le Page, E. J. Gabe and K. U. Ingold, *J. Am. Chem. Soc.*, 2002, **102**, 7791–7792.

20 T. Doba, G. W. Burton and K. U. Ingold, *J. Am. Chem. Soc.*, 2002, **105**, 6505–6506.
21 M. Lucarini, G. F. Pedulli and M. Cipollone, *J. Org. Chem.*, 2002, **59**, 5063–5070.
22 H. A. Zahalka, B. Robillard, L. Hughes, J. Lusztyk, G. W. Burton, E. G. Janzen, Y. Kotake and K. U. Ingold, *J. Org. Chem.*, 2002, **53**, 3739–3745.
23 B. Robillard, L. Hughes, M. Slaby, D. A. Lindsay and K. U. Ingold, *J. Org. Chem.*, 2002, **51**, 1700–1704.
24 J. Malmstrom, M. Jonsson, I. A. Cotgreave, L. Hammarstrom, M. Sjodin and L. Engman, *J. Am. Chem. Soc.*, 2001, **123**, 3434–3440.
25 D. Shanks, R. Amorati, M. G. Fumo, G. F. Pedulli, L. Valgimigli and L. Engman, *J. Org. Chem.*, 2006, **71**, 1033–1038.
26 R. Amorati, A. Cavalli, M. G. Fumo, M. Masetti, S. Menichetti, C. Pagliuca, G. F. Pedulli and C. Viglianisi, *Chem. – Eur. J.*, 2007, **13**, 8223–8230.
27 S. Menichetti, R. Amorati, M. G. Bartolozzi, G. F. Pedulli, A. Salvini and C. Viglianisi, *Eur. J. Org. Chem.*, 2010, 2218–2225.
28 R. Amorati, L. Valgimigli, P. Diner, K. Bakhtiari, M. Saeedi and L. Engman, *Chem. – Eur. J.*, 2013, **19**, 7510–7522.
29 J. F. Poon, V. P. Singh, J. Yan and L. Engman, *Chem. – Eur. J.*, 2015, **21**, 2447–2457.
30 D. Tanini, L. Panzella, R. Amorati, A. Capperucci, E. Pizzo, A. Napolitano, S. Menichetti and M. d'Ischia, *Org. Biomol. Chem.*, 2015, **13**, 5757–5764.
31 C. Viglianisi, K. Vasa, D. Tanini, A. Capperucci, R. Amorati, L. Valgimigli, A. Baschieri and S. Menichetti, *Chem. – Eur. J.*, 2019, **25**, 9108–9116.
32 C. Viglianisi and S. Menichetti, *Antioxidants*, 2019, **8**, 487.
33 R. Amorati, F. Catarzi, S. Menichetti, G. F. Pedulli and C. Viglianisi, *J. Am. Chem. Soc.*, 2008, **130**, 237–244.
34 T. Schaefer, T. A. Wildman and S. R. Salman, *J. Am. Chem. Soc.*, 2002, **102**, 107–110.
35 R. Amorati, M. G. Fumo, S. Menichetti, V. Mugnaini and G. F. Pedulli, *J. Org. Chem.*, 2006, **71**, 6325–6332.
36 D. L. Howard and H. G. Kjaergaard, *Phys. Chem. Chem. Phys.*, 2008, **10**, 4113–4118.
37 C. Viglianisi, M. G. Bartolozzi, G. F. Pedulli, R. Amorati and S. Menichetti, *Chem. – Eur. J.*, 2011, **17**, 12396–12404.
38 C. Viglianisi, R. Amorati, L. Di Pietro and S. Menichetti, *Chem. – Eur. J.*, 2015, **21**, 16639–16645.
39 C. Viglianisi, L. D. Pietro, V. Meoni, R. Amorati and S. Menichetti, *ARKIVOC*, 2019, **2019**, 65–85.
40 S. Menichetti, R. Amorati, V. Meoni, L. Tofani, G. Caminati and C. Viglianisi, *Org. Lett.*, 2016, **18**, 5464–5467.
41 P. Politzer, J. S. Murray and T. Clark, *Phys. Chem. Chem. Phys.*, 2013, **15**, 11178–11189.
42 J. S. Murray, P. Lane, T. Clark and P. Politzer, *J. Mol. Model.*, 2007, **13**, 1033–1038.
43 B. R. Beno, K. S. Yeung, M. D. Bartberger, L. D. Pennington and N. A. Meanwell, *J. Med. Chem.*, 2015, **58**, 4383–4438.
44 R. J. Fick, G. M. Kroner, B. Nepal, R. Magnani, S. Horowitz, R. L. Houtz, S. Scheiner and R. C. Trievel, *ACS Chem. Biol.*, 2016, **11**, 748–754.
45 M. Turbiez, P. Frere, M. Allain, C. Videlot, J. Ackermann and J. Roncali, *Chem. – Eur. J.*, 2005, **11**, 3742–3752.
46 J. S. Murray, P. Lane and P. Politzer, *Int. J. Quantum Chem.*, 2008, **108**, 2770–2781.
47 J. Fanfrlik, A. Prada, Z. Padelkova, A. Pecina, J. Machacek, M. Lepsik, J. Holub, A. Ruzicka, D. Hnyk and P. Hobza, *Angew. Chem., Int. Ed.*, 2014, **53**, 10139–10142.
48 M. Zandomeneghi, L. Carbonaro and C. Caffarata, *J. Agric. Food Chem.*, 2005, **53**, 759–766.
49 G. Neunert, P. Polewski, P. Walejko, M. Markiewicz, S. Witkowski and K. Polewski, *Spectrochim. Acta, Part A*, 2009, **73**, 301–308.
50 T. Verleyen, R. Verhe, L. Garcia, K. Dewettinck, A. Huyghebaert and W. De Greyt, *J. Chromatogr. A*, 2001, **921**, 277–285.
51 S. L. Abidi and K. A. Rennick, *J. Chromatogr. A*, 2001, **913**, 379–386.
52 S. L. Curto, G. Dugo, L. Mondello, G. Errante and M. Russo, *Ital. J. Food Sci.*, 2001, **13**, 221–228.
53 A. Sanchez-Perez, M. M. Delgado-Zamarreno, M. Bustamante-Rangel and J. Hernandez-Mendez, *J. Chromatogr. A*, 2000, **881**, 229–241.
54 M. Tasioula-Margari and O. Okogeri, *Food Chem.*, 2001, **74**, 377–383.
55 T. G. Diaz, I. Duran-Meras, M. I. Rodríguez Cáceres and B. R. Murillo, *Appl. Spectrosc.*, 2006, **60**, 194–202.
56 A. Patel, S. Böhmdorfer, A. Hofinger, T. Netscher and T. Rosenau, *Eur. J. Org. Chem.*, 2009, 4873–4881.
57 G. Viault, M. Kempf, A. Ville, K. Alsabil, R. Perrot, P. Richomme, J. J. Helesbeux and D. Seraphin, *ChemMedChem*, 2021, **16**, 881–890.
58 K. Mitsudo, Y. Kobashi, K. Nakata, Y. Kurimoto, E. Sato, H. Mandai and S. Suga, *Org. Lett.*, 2021, **23**, 4322–4326.
59 G. W. Burton, T. Doba, E. Gabe, L. Hughes, F. L. Lee, L. Prasad and K. U. Ingold, *J. Am. Chem. Soc.*, 2002, **107**, 7053–7065.
60 C. Viglianisi, V. Di Pilla, S. Menichetti, V. M. Rotello, G. Candiani, C. Malloggi and R. Amorati, *Chem. – Eur. J.*, 2014, **20**, 6857–6860.
61 R. Amorati, A. Baschieri and L. Valgimigli, *J. Chem.*, 2017, **2017**, 1–12.
62 R. Amorati, S. Menichetti, C. Viglianisi and M. C. Foti, *Chem. Commun.*, 2012, **48**, 11904–11906.
63 K. A. Harrison, E. A. Haidasz, M. Griesser and D. A. Pratt, *Chem. Sci.*, 2018, **9**, 6068–6079.
64 A. Baschieri, L. Pulvirenti, V. Muccilli, R. Amorati and C. Tringali, *Org. Biomol. Chem.*, 2017, **15**, 6177–6184.
65 R. Amorati, J. Zotova, A. Baschieri and L. Valgimigli, *J. Org. Chem.*, 2015, **80**, 10651–10659.
66 R. Amorati, L. Valgimigli, L. Panzella, A. Napolitano and M. d'Ischia, *J. Org. Chem.*, 2013, **78**, 9857–9864.
67 M. Montalti, A. Credi, L. Prodi and M. T. Gandolfi, *Handbook of Photochemistry*, 2006.
68 R. Amorati and L. Valgimigli, *Free Radical Res.*, 2015, **49**, 633–649.

69 R. Amorati, P. T. Lynett, L. Valgimigli and D. A. Pratt, *Chem. – Eur. J.*, 2012, **18**, 6370–6379.
70 P. Mulder, H. G. Korth, D. A. Pratt, G. A. DiLabio, L. Valgimigli, G. F. Pedulli and K. U. Ingold, *J. Phys. Chem. A*, 2005, **109**, 2647–2655.
71 M. Lucarini, P. Pedrielli, G. F. Pedulli, S. Cabiddu and C. Fattuoni, *J. Org. Chem.*, 1996, **61**, 9259–9263.
72 G. A. Crosby and J. N. Demas, *J. Phys. Chem.*, 2002, **75**, 991–1024.
73 S. R. Meech and D. Phillips, *J. Photochem.*, 1983, **23**, 193–217.